

Magnetic Properties of an Amorphous Mn-P-C Alloy*

Ryusuke Hasegawa

*W. M. Keck Laboratory of Engineering Materials, California Institute of Technology,
Pasadena, California 91109*

(Received 16 September 1970)

The magnetic properties of an amorphous $\text{Mn}_{75}\text{P}_{15}\text{C}_{10}$ alloy obtained by rapid quenching from the liquid state and those of the crystalline alloy of the same composition have been measured. The results are interpreted by assuming that the amorphous alloy consists of three different regions mixed randomly (called phases for simplicity) in which the local atomic arrangements are different. Both magnetic and x-ray analyses indicate that one of these phases has a local order based on crystalline Mn_3P . One of the remaining phases could have a local order of a Mn_5C_2 type, but the other phase cannot be described in detail. Evidence is shown that the antiferromagnetic Néel temperature of an amorphous alloy is reduced to about $\frac{1}{2}$ of that of the corresponding crystalline alloy. By using molecular-field analysis, present results show that the magnetic interactions are less localized to the first-nearest neighbors in the amorphous Mn_3P phase than in the crystalline phase.

INTRODUCTION

As predicted by Gubanov,¹ a number of amorphous ferromagnets have been found.²⁻¹⁰ Gubanov's results imply that, upon transition from a crystalline to noncrystalline state, the values of the magnetization and the Curie temperature of a ferromagnet increase or decrease depending on the increase or decrease of the size of the d - d exchange integral. It has been suggested also that some nonferromagnetic crystalline materials would become ferromagnetic upon transition to an amorphous state. These arguments are based on the fact that the interatomic distances are larger in the amorphous than in the crystalline alloy. The experimental results reported so far, however, indicate that the values of the magnetization and of the Curie temperature are always smaller in amorphous materials than in the corresponding crystalline materials, and this is consistent with the results of Handrich.¹¹ There has been no evidence of an amorphous ferromagnet which is not ferromagnetic in its crystalline state.

An amorphous $\text{Mn}_{75}\text{P}_{15}\text{C}_{10}$ alloy was obtained by Lin¹² by rapid quenching from the liquid state. This alloy is analogous to the amorphous $\text{Fe}_{75}\text{P}_{15}\text{C}_{10}$ which has been studied in detail.^{6,13-16} The study¹⁴ of the amorphous Fe-P-C alloy indicates that the local atomic arrangement in this alloy can be described by a randomized bcc Fe lattice. However, when the amorphous Fe-P-C alloy is transformed into a crystalline state at a very high rate of heating (above 300 °C/min), the equilibrium phases are divided into about 56% Fe_3P , 37% Fe_5C_2 , and 7% Fe.¹⁷ This implies that the amorphous Fe-P-C alloy could have a local order of these structures mixed randomly. Since the x-ray diffraction patterns of amorphous $\text{Fe}_{75}\text{P}_{15}\text{C}_{10}$ and $\text{Mn}_{75}\text{P}_{15}\text{C}_{10}$ are

very similar, it is probable that the local order is the same in the two amorphous alloys. If this is the case, the local structure of the amorphous Mn-P-C alloy could be mainly of a Mn_3P type. The two isostructural crystalline phases Fe_3P and Mn_3P differ in their properties, since Fe_3P is ferromagnetic with a Curie temperature of 716 °K,¹⁸ and Mn_3P is antiferromagnetic with a Néel temperature of 115 °K.¹⁹ A Curie-Weiss plot for the amorphous $\text{Mn}_{75}\text{P}_{15}\text{C}_{10}$ ²⁰ shows a curvature which is concave toward the temperature axis, and the magnetization curve has an antiferromagnetic peak at around 15 °K. From these results, Sinha²⁰ concluded that the magnetic behavior of the Mn-P-C amorphous alloy is due to the coexistence of ferri- and antiferromagnetic regions. The purpose of the present study is to understand the complex magnetic properties of the amorphous Mn-P-C alloy.

EXPERIMENTAL RESULTS

The amorphous $\text{Mn}_{75}\text{P}_{15}\text{C}_{10}$ alloy was prepared according to the method described in Ref. 20. The magnetic moments were measured over a temperature range 4.2–300 °K and in fields up to 8.40 kOe. The amorphous alloy was then crystallized by annealing at 800 °C for 1 h, and the magnetic measurements were made on the crystalline alloy. In both the amorphous and the crystalline case, the magnetic moments were proportional to the applied magnetic field at all temperatures. The susceptibilities χ obtained from these data are presented in the form of $1/\chi$ vs T in Fig. 1.

A Debye-Scherrer pattern of the crystalline alloy was obtained with Cr $K\alpha$ radiation. The results of the θ values are given in Table I together with those for a crystalline Mn_3P alloy²¹ and those for a crystalline Mn_5C_2 alloy.²² A comparison of

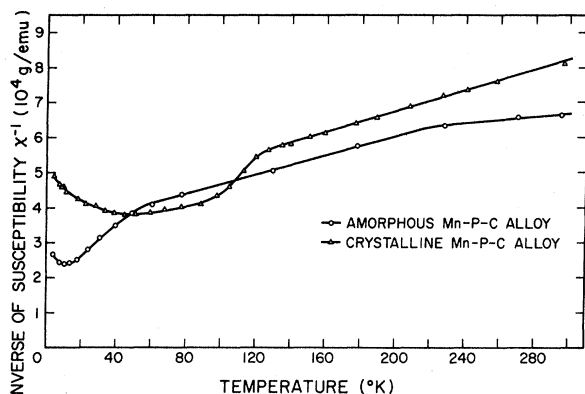


FIG. 1. Inverse of the magnetic susceptibility per gram of an amorphous and a crystalline $\text{Mn}_{75}\text{P}_{15}\text{C}_{10}$ alloy. The crystalline alloy was obtained by annealing the amorphous alloy at 800°C for 1 h.

the three sets of θ values (Table I) leads to the conclusion that most of the observed lines for the crystalline Mn-P-C alloy can be identified as those of Mn_3P . Several weak lines marked with an asterisk (Table I) could be indexed as those of the monoclinic Mn_5C_2 structure. It is probable that the remaining reflection (e.g., line 3) is due to small amounts of one of several manganese carbides.

DISCUSSION AND CONCLUSIONS

The $1/\chi$ -vs- T plot for the amorphous Mn-P-C alloy (Fig. 1) can be considered as a superposition of three curves, each of which exhibits paramagnetic and antiferromagnetic behavior at high and low temperatures, respectively. Within this assumption, the observed susceptibility can be written as

$$\chi_1 = \frac{C}{(T + \theta_N)} \quad \text{for } T_1 \leq T \leq 300^\circ\text{K},$$

$$\chi_i = \frac{[\chi_{i-1}(T_{i-1})](T_{i-1} + \theta_{N_i})}{(T + \theta_{N_i})}$$

$$\text{for } i = 2 \text{ and } 3 \text{ and } T_{i+1} < T < T_i,$$

where C is the Curie constant and θ_{N_i} is the paramagnetic Néel temperature. The values of θ_{N_i} , T_i , and the magnetic moments calculated from the slope of $1/\chi$ vs T are listed in Table II. The change in the slope of $1/\chi$ -vs- T plot at T_1 and T_2 indicates that the region I ($i=1$) with a large moment is the smallest in its volume followed by the region II ($i=2$) with a smaller moment and by the region III ($i=3$) with the smallest moment. The temperatures T_1 and T_2 are probably the antiferromagnetic Néel temperatures for the regions I and II, respectively.

The Néel temperature for the region III is 10.5°K , which is clearly shown in Fig. 1.

The susceptibility for the crystalline Mn-P-C alloy obeys the Curie-Weiss law above 120°K (Fig. 1), and this gives the magnetic moment μ ($=gS$) of $1.14 \mu_B/\text{Mn atom}$ with a paramagnetic Néel temperature θ_N of 250°K . On the other hand, if 45 at. % of Mn react with the 15-at. % P to result in a crystalline Mn_3P phase as evidenced in the x-ray data, the result of the Curie-Weiss analysis gives $\mu = 1.48 \mu_B/\text{Mn atom}$, this value being close to that ($\mu = 1.68 \mu_B$) obtained by Gambino *et al.*¹⁹ for crystalline Mn_3P . The temperature (120°K) at which the susceptibility deviates from the Curie-Weiss law is very close to the Néel temperature ($=115^\circ\text{K}$) obtained for crystalline Mn_3P .¹⁹ The results of the x-ray analysis and the magnetic data lead to the conclusion that the observed magnetic susceptibility (for $120^\circ\text{K} < T < 300^\circ\text{K}$) of the crystalline Mn-P-C alloy is probably due to the existence of a crystalline Mn_3P phase. Below 120°K , the susceptibility deviates from the Curie-Weiss law and undergoes a maximum at about 50°K . This behavior is probably due to the existence of some antiferromagnetic phases (possibly of Mn carbides), one of which could be a Mn_5C_2 type as the x-ray data suggest.

A comparison of the results obtained for the amorphous and crystalline Mn-P-C alloys leads to several interesting conclusions. The atomic arrangement in the amorphous Mn-P-C alloy consists of three different types of local order which might be called phases.²³ These phases have local order (over several atomic spacings) and are randomly mixed. Each of these phases shows paramagnetic and antiferromagnetic behavior at high and low temperatures, respectively. The phase which corresponds to the region I (see Table II) could not be observed in the crystalline alloy. This is probably due to a high Néel temperature (possibly between 400 and 500°K) of this phase in the crystalline case. The closeness of the slope of $1/\chi$ vs T for the region II to that for the crystalline alloy ($T > 120^\circ\text{K}$) suggests that the susceptibility of the amorphous alloy for $50^\circ\text{K} < T < 220^\circ\text{K}$ is probably due to the short-range ordering of a Mn_3P type in the amorphous alloy. The magnetic data below 50°K for the amorphous alloy are probably to be compared with those below 120°K for the crystalline alloy. It is noticed that the antiferromagnetic Néel temperature is reduced from 50 to 10.5°K upon transition from a crystalline to an amorphous state. A similar phenomenon is observed for the Mn_3P phase whose Néel temperature is reduced from 120 to $(50 \pm 10)^\circ\text{K}$. These results indicate that the Néel temperature decreases by about 50% upon transition from a crystalline to an amorphous state in analogy to the similar decrease of the ferro-

TABLE I. X-ray data for the crystalline Mn-P-C alloy, Mn_3C_2 phases ($\text{CrK}\alpha$ radiation).

Crystalline Mn-P-C alloy			Mn_3P phase (Ref. 21), or Mn_5C_2 phase* (Ref. 22)		
Line	Visual intensity ^a	θ (degree)	$\{hkl\}$	Relative intensity ^b	θ (degree)
1	vw	26.76	$\{301\}$	25.16	26.761
2*	vw	28.01	$\{311\}$	0.98	28.05
3 ^c	vw	28.95			
4	vw	30.17	$\{002\}$	1.63	30.081
5	s	31.01	$\left\{ \begin{matrix} \{321\} \\ \{231\} \end{matrix} \right\}$	$\left\{ \begin{matrix} 90.07 \\ 65.56 \end{matrix} \right\}$	30.979
6	s	32.04	$\left\{ \begin{matrix} \{330\} \\ \{112\} \end{matrix} \right\}$	$\left\{ \begin{matrix} 40.00 \\ 89.03 \end{matrix} \right\}$	$\left\{ \begin{matrix} 31.940 \\ 32.096 \end{matrix} \right\}$
7*	vvw	32.66	$\left\{ \begin{matrix} \{220\} \\ \{112\} \end{matrix} \right\}$	$\left\{ \begin{matrix} 0.05 \\ 1.37 \end{matrix} \right\}$	$\left\{ \begin{matrix} 32.60 \\ 32.68 \end{matrix} \right\}$
8*	w	33.44	$\{021\}$	5.71	33.37
9	m	33.84	$\left\{ \begin{matrix} \{420\} \\ \{240\} \end{matrix} \right\}$	$\left\{ \begin{matrix} 59.51 \\ 1.49 \end{matrix} \right\}$	33.893
10*	w	34.27	$\left\{ \begin{matrix} \{40\bar{2}\} \\ \{31\bar{2}\} \end{matrix} \right\}$	$\left\{ \begin{matrix} 2.11 \\ 3.65 \end{matrix} \right\}$	$\left\{ \begin{matrix} 34.17 \\ 34.53 \end{matrix} \right\}$
11	ms	34.82	$\left\{ \begin{matrix} \{411\} \\ \{141\} \end{matrix} \right\}$	$\left\{ \begin{matrix} 34.14 \\ 100.00 \end{matrix} \right\}$	34.887
12	vvw	...			
13*	vw	36.50	$\left\{ \begin{matrix} \{600\} \\ \{221\} \end{matrix} \right\}$	$\left\{ \begin{matrix} 0.50 \\ 2.82 \end{matrix} \right\}$	$\left\{ \begin{matrix} 36.50 \\ 36.52 \end{matrix} \right\}$
14	m	37.73	$\{222\}$	41.55	37.798
15*	vw	38.73	$\left\{ \begin{matrix} \{511\} \\ \{312\} \end{matrix} \right\}$	$\left\{ \begin{matrix} 2.15 \\ 3.22 \end{matrix} \right\}$	$\left\{ \begin{matrix} 38.58 \\ 38.90 \end{matrix} \right\}$
16	ms	39.49	$\left\{ \begin{matrix} \{510\} \\ \{150\} \end{matrix} \right\}$	$\left\{ \begin{matrix} 0.61 \\ 41.14 \end{matrix} \right\}$	39.480
17*	vw	40.57	$\left\{ \begin{matrix} \{402\} \\ \{42\bar{1}\} \end{matrix} \right\}$	$\left\{ \begin{matrix} 2.66 \\ 2.00 \end{matrix} \right\}$	$\left\{ \begin{matrix} 39.96 \\ 40.30 \end{matrix} \right\}$
18	vw	42.12	$\left\{ \begin{matrix} \{431\} \\ \{341\} \end{matrix} \right\}$	$\left\{ \begin{matrix} 4.12 \\ 7.58 \end{matrix} \right\}$	42.218

^avvw = very very weak, w = weak, m = medium, ms = medium strong, and s = strong.

^bRelative intensity should be compared within the same

phase.

^cCould not be identified.

magnetic Curie temperature in amorphous ferromagnets.² This explains the fact that the crystalline phase corresponding to the region I could not be observed in the present temperature range ($4.2^\circ\text{K} \leq T < 300^\circ\text{K}$). One probably has to extend the temperature range up to above 450°K to observe this phase magnetically. In the light of the two-sublattice model,²⁴ the ratio $\theta_N/T_N = (A + \Gamma)/(A - \Gamma)$ is 5 and 2.1 for the amorphous and the crystalline Mn_3P phase, respectively. This indicates that the ratio of the molecular-field coefficient for the first-nearest-neighbor interaction (A) to that for the second-nearest-neighbor interaction (Γ) is 1.5 and 2.8 for the amorphous and the crystalline phase, respectively. This suggests

that magnetic interactions are less localized at the first-nearest neighbors in the amorphous Mn_3P phase than in its crystalline phase.

In summary, we conclude that the amorphous Mn-P-C alloy probably consists of three different phases mixed randomly, each of which is para-

TABLE II. Results of the magnetic measurements for the amorphous Mn-P-C alloy.

Region	T_i ($^\circ\text{K}$)	θ_{N_i} ($^\circ\text{K}$)	$\mu_i (= gS\mu_B/\text{Mn atom})$
I ($i=1$)	220 ± 5	1090	2.29
II ($i=2$)	50 ± 10	250	1.14
III ($i=3$)	25	35	0.42

magnetic at high temperatures and becomes anti-ferromagnetic at low temperatures. One of the three phases could be identified as a Mn_3P type. The x-ray data show that one of the other two could have a structure based on Mn_5C_2 . The remaining phase is unknown at the present moment and is possibly one of the Mn carbides. These results differ from the previous conclusion²⁰ that the amorphous alloy is a mixture of antiferro- and ferromagnetic regions. It is also found that the anti-ferromagnetic Néel temperature of an amorphous phase is about $\frac{1}{2}$ of that of the corresponding crystalline counterpart. Finally, in the molecular-field model, present results show that the magnetic interactions in the amorphous Mn_3P phase are less

localized to the first-nearest neighbors compared with that in the crystalline phase.

ACKNOWLEDGMENTS

It is a pleasure to acknowledge the useful advice of Professor Pol Duwez. The author is indebted to Dr. S. C. H. Lin, of Varian Associates, who interested him in the present study and also to Dr. S. Rundqvist, of Uppsala University, who kindly has supplied the author with x-ray data for MnP , Mn_2P , and Mn_3P alloys and has pointed out the possibility of the presence of Mn_5C_2 lines in our x-ray data. Discussions with Dr. A. K. Sinha of Bell Telephone Laboratories were very stimulating.

*Work supported by the U. S. Atomic Energy Commission.

¹A. I. Gubanov, *Fiz. Tverd. Tela* **2**, 502 (1960) [*Soviet Phys. Solid State* **2**, 468 (1960)].

²For a review of amorphous ferromagnets, see R. Hasegawa, *Solid State Phys. (Japan)* **5**, 63 (1970) (in Japanese).

³S. Mader and A. S. Nowick, *Appl. Phys. Letters* **7**, 57 (1965).

⁴B. G. Bagley and D. Turnbull, *Bull. Am. Phys. Soc.* **10**, 1101 (1965).

⁵C. C. Tsuei and Pol Duwez, *J. Appl. Phys.* **37**, 435 (1966).

⁶Pol Duwez and S. C. H. Lin, *J. Appl. Phys.* **38**, 4096 (1967).

⁷V. V. Bondar', K. M. Gorbunova, and Yu M. Polukarov, *Fiz. Metal. Metalloved.* **26**, 568 (1968).

⁸K. Tamura and H. Endo, *Phys. Letters* **29A**, 52 (1969).

⁹P. L. Maitrepierre, Ph.D. thesis, California Institute of Technology, 1969 (unpublished).

¹⁰R. Hasegawa, *J. Appl. Phys.* **41**, 4096 (1970).

¹¹K. Handrich, *Phys. Status Solidi* **32**, K55 (1969).

¹²S. C. H. Lin (private communication).

¹³C. C. Tsuei, G. Longworth, and S. C. H. Lin, *Phys. Rev.* **170**, 603 (1968).

¹⁴S. C. H. Lin and Pol Duwez, *Phys. Status Solidi* **34**, 469 (1969).

¹⁵S. C. H. Lin, *J. Appl. Phys.* **40**, 2173 (1969).

¹⁶S. C. H. Lin, *J. Appl. Phys.* **40**, 2175 (1969).

¹⁷P. K. Rastogi and Pol Duwez, *J. Non-Cryst. Solids* **5**, 1 (1970).

¹⁸A. J. P. Meyer and M. C. Cadeville, *J. Phys. Soc. Japan* **17**, Suppl. B1 (1962).

¹⁹R. J. Gambino, T. R. McGuire, and Y. Nakamura, *J. Appl. Phys.* **38**, 1253 (1967).

²⁰A. K. Sinha, *J. Appl. Phys.* (to be published).

²¹S. Rundqvist (private communication); also see *Acta Chem. Scand.* **16**, 992 (1962).

²²E. Stenberg, *Acta Chem. Scand.* **15**, 861 (1961).

²³A mixture of amorphous phases similar to the present case has been found in amorphous silicon monoxides; see, for example, S. C. H. Lin and M. Joshi, *J. Electrochem. Soc.* **116**, 1740 (1969).

²⁴See, for example, A. J. Dekker, *Solid State Physics* (Prentice-Hall, Englewood Cliffs, N. J., 1957), p. 484.

Changes in the Thermodynamic Character of the NH_4Cl Order-Disorder Transition at High Pressures*

Carl W. Garland and Bruce B. Weiner†

Department of Chemistry and Center for Materials Science and Engineering, Massachusetts Institute of Technology, Cambridge, Massachusetts 02139

(Received 23 September 1970)

Variations in the length L of an NH_4Cl crystal in the vicinity of its order-disorder transition line have been determined with a capacitance method. At low pressures, there is a small first-order discontinuity ΔL superimposed on a λ -like variation in L . At a "critical point" near 255.75°K and 1493 bar, L varies continuously but κ_T and α appear to diverge. At higher pressures, the variation in L at the transition becomes progressively more gradual.

The order-disorder transition in NH_4Cl , which involves the relative orientations of the tetrahedral NH_4^+ ions in a CsCl -type cubic structure, is in

many ways analogous to the ferromagnetic transition in a compressible Ising lattice. In the case of NH_4Cl , mechanical variables play an important